were selected by an immunoassay (ELISA)[20] against a conjugate of **1** with bovine albumin. Antibody of IgG class was obtained by propagating selected clones in mouse (Balb/c 129G1X$^+$) ascites. Purified[1] mAb was dialyzed against phosphate buffer (20 mM, pH 7.0), and its protein concentration was determined by the BCA method (Pierce). An aliquot of the antibody stock solution, calculated to give 0.5 μM protein, was added to a solution of the ester or carbonate (10 μM) and an internal standard (acetophenone, 20 μM) in phosphate buffer (50 mM, pH 8.0). The mixture was kept at 23 °C and analyzed by HPLC as previously described.[2]

Kinetic Measurements and Data Analysis. Esterolysis rates were measured by absorbance changes at 290 nm on a Cary 14DS that is digitally interfaced to an AT+T personal computer as supplied by AVIV Corp. (Lakewood, NJ). Reactions were performed in 1.00 mL of buffer solution in a quartz cuvette maintained at 25.0 ± 0.1 °C by a water-jacketed cell holder equilibrated to a Lauda RM6 circulating water bath.

The initial linear rate was measured at <3% hydrolysis of total substrate. The observed rate was corrected for the uncatalyzed rate of hydrolysis in the absence of antibody. Kinetic parameters V_{max} and K_m were determined by nonlinear least-squares fitting of the initial rate vs substrate concentration to a hyperbolic curve described by the Michaelis-Menten equation. The inhibition constant K_i was extrapolated from a replot of the slopes of the linear Henderson plots vs total substrate concentration. The variation of initial rates as a function of pH was measured in borate (50 mM) at pH above 8.5 and in Tricine (100 mM) otherwise. The pK_a that describes the pH dependence of k_{cat} vs hydrogen ion concentration was determined by fitting the data to eq 1, where

$$k_{cat}(H) = k_{cat}K_a/(K_a + [H^+]) \quad (1)$$

$k_{cat}(H)$ is the turnover rate at a given pH, k_{cat} is the limiting k_{cat} at high pH, K_a is the ionization constant for a single titrable amino acid side chain, and $[H^+]$ is the hydrogen ion concentration.

Chemical Modification of mAb 50D8. An aliquot of tetranitromethane in dioxane (200 mM), calculated to give 2.0 mM (100 equiv), was added to a solution of antibody (20.0 μM) in Tris buffer (100 mM, pH 8.0) at 23 °C. The activity was checked periodically by addition of an aliquot of this solution to a solution of **7** (0.60 mM) in borate buffer (50 mM, pH 9.2) and the initial rate determined spectrophotometrically. After 1 h the mixture was separated by HPLC on size-exclusion gel (TSK gel G2000SW, Phenomenex), eluting with Tris buffer (100 mM, pH 8.0). The protein was collected and concentrated, and its specific absorbance at 428 nm and protein concentration was determined. In a second experiment antibody was preincubated with **2** (0.14 mM) for 30 min and then subjected to tetranitromethane treatment as before.

A similar procedure was used for treating the protein (6.0 μM) with iodoacetamide (10.0 mM) of diethyl pyrocarbonate (0.60 mM), and activity was monitored as a function of reaction time.

Production of Fab Fragment. A mixture of antibody (10 mg) and immobilized papain on 6% beaded agarose (0.5 mL of commercial slurry; Pierce) in 100 mM phosphate, 20 mM cysteine hydrochloride buffer (1.0 mL) was adjusted to pH 7.0 ± 0.2 and shaken for 8 h at 37 °C. Reaction progress was checked by SDS-Page[21] (10-15% gel), using the Pharmacia pHast system. Immobilized enzyme was removed by filtration through a 50-μm filter, and the filtrate was passed through a prepacked protein A-Sepharose column with the recommended buffers (Pierce "immunopure" kit). The esterase activity of the effluent was assayed by the HPLC method described.

Acknowledgment. We acknowledge the expert technical assistance of Diane Schloeder and Sheri Hunt. This work was supported by the National Institutes of Health (Grant GM-35318) and the National Science Foundation (Grant DCB-8607352).

(19) Niman, H. L.; Elder, J. H. In *Monoclonal Antibodies and T-Cell Products*; Katz, D. H., Ed.; CRC: Boca Raton, FL, 1982; pp 23-51.
(20) Engvall, E.; Perlmann, P. *J. Immunol.* **1972**, *109*, 129.
(21) Laemmli, U. *Nature (London)* **1970**, *227*, 680.

Specific Ring Stacking Interaction on the Tryptophan-7-Methylguanine System: Comparative Crystallographic Studies of Indole Derivatives-7-Methylguanine Base, Nucleoside, and Nucleotide Complexes[1]

Toshimasa Ishida,*[2a] Mitsunobu Doi,[2a] Hitoshi Ueda,[2a] Masatoshi Inoue,[2a] and George M. Scheldrick[2b]

Contribution from the Laboratory of Physical Chemistry, Osaka University of Pharmaceutical Sciences, 2-10-65 Kawai, Matsubara, Osaka 580, Japan, and Anorganisch-Chemisches Institut der Universität Göttingen, Tammannstrasse 4, 3400 Göttingen, FRG. *Received June 22, 1987*

Abstract: For a comparative interaction study between the protonated or methylated guanine base in nucleic acid and the tryptophan residue in protein, three model complexes, 7-methyl-9-ethylguanine (m^{7}GuA)-indole-3-acetic acid (IAA), 7-methylguanosine (m^{7}GuO)-indole-3-acetic acid (IAA), and 7-methylguanosine 5'-monophosphate (m^{7}GMP)-tryptamine (TRP), were subjected to X-ray crystal analyses. All crystals formed extensive stacking layers consisting of alternating guanine and indole rings. These ring-ring interactions are all characterized by nearly parallel alignments of both aromatic rings and by interplanar spacing in the vicinity of 3.4 Å. However, these stacking interaction modes were significantly affected by the ribose and phosphate groups, and the overlapping area of both rings was in the order of m^{7}GMP ≥ m^{7}GuO > m^{7}GuA. In particular, some stacking pairs in m^{7}GuO-IAA and m^{7}GMP-TRP complexes showed the existence of partial π charge transfer from the indole ring to the guanine base in their ground states. The present results clearly show the importance of the tryptophan residue in protein for the selective recognition of the protonated or methylated guanine base in nucleic acid. Furthermore, the results shed light on the recognition mechanism of cap binding protein for the mRNA cap structure.

The ability of a protein to recognize a specific sequence of bases along a strand of DNA or RNA is a fundamental biological process, which is guaranteed by the specific interactions between their constituent chemical growth groups, as well as by the complementary spatial structure between these macromolecules. Therefore, information concerning the interaction geometries is of great significance for understanding the mechanism of selective recognition.

Aromatic amino acids can bind with nucleic bases via π-π stacking interaction.[3] Among them, tryptophan has the strongest binding ability because of the best π-electron donation character

(1) Part 20: Structural Studies of the Interaction between Indole Derivatives and Biologically Important Aromatic Compounds.
(2) (a) Osaka University of Pharmaceutical Sciences. (b) Anorganishch-Chemisches Institut der Universität Göttingen.

0002-7863/88/1510-2286$01.50/0

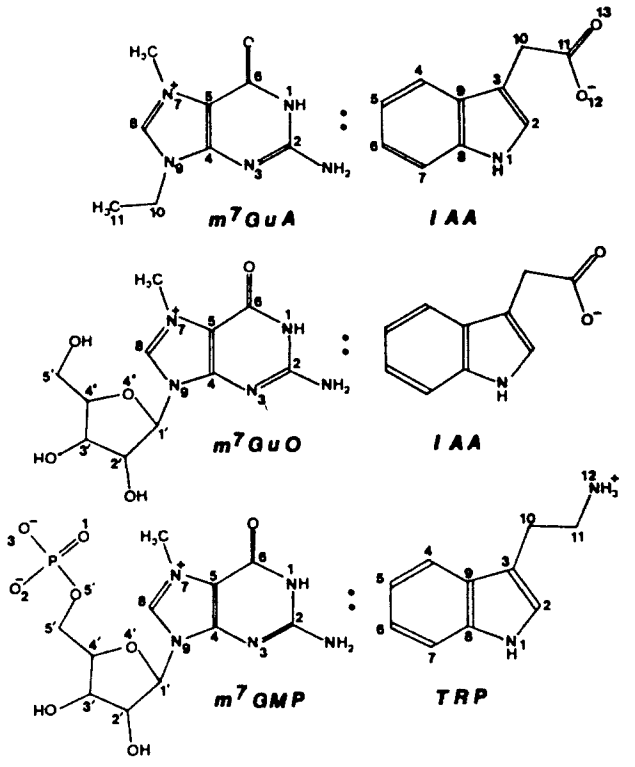

Figure 1. Chemical formulas and atomic numberings used for X-ray analyses.

of the indole ring at its side chain,[4] and many solution studies on this interaction have been done by using various spectroscopic methods. But, clear-cut presentations of stacking interactions in the crystalline state are very meager. This is mainly due to the weakness of such an interaction force.

Generally, the stacking interaction arises from the interaction between the π orbitals of two aromatic rings, especially between the highest occupied molecular orbital (HOMO) of the donor ring and the lowest unoccupied molecular orbital (LUMO) of the acceptor ring. We have already shown, using an indole–adenine system,[5] that the LUMO energy is lowered by the protonation or methylation of the nucleic base, leading to reinforcement of the HOMO–LUMO interaction. This implies that if the nucleic bases are protonated or methylated, the stacking interaction becomes important in the nucleic acid–protein interaction. Recently, the importance of nucleic acid methylation has been discussed in relation to biological processes. Therefore, it is of interest to know to what extent the stacking interaction is strengthened by base methylation.

7-Methylguanine (m^7G) is not only a major product of nucleic acid methylation[6] but also an important component characterizing the "cap" structure, $m^7G(5')ppp(5')N$, of eukaryotic mRNA.[7] Therefore, study of the m^7G–tryptophan interaction is important for considering the biological implications of m^7G, in addition to the above-mentioned reasons. Although the interactions essentially take place between the aromatic rings, they are largely affected by the side chains. In order to determine the characteristics of the interaction exactly, therefore, a comparative study on the tryptophan–m^7G (base, nucleoside, nucleotide) systems is necessary.

Table I. Summary of Crystal Data and Intensity Collection

	m^7GuA–IAA	m^7GuO–IAA	m^7GMP–TRP
formula	$C_8H_{12}N_5O^+ \cdot C_{10}H_8NO_2^-$	$C_{11}H_{16}N_5O_5^+ \cdot C_{10}H_8NO_2 \cdot 2H_2O$	$C_{11}H_{15}N_5O_8P^- \cdot C_{10}H_{13}N_2^+ \cdot 3H_2O$
FW	368.39	490.47	591.51
crystal system	monoclinic	monoclinic	triclinic
space group	$P2_1$	$P2_1$	$P1$
a, Å	7.460 (2)	6.803 (1)	6.741 (3)
b, Å	28.581 (7)	13.738 (3)	7.584 (4)
c, Å	8.611 (2)	23.430 (7)	12.904 (6)
α, deg	90	90	97.32 (12)
β, deg	95.90 (3)	97.15 (5)	80.95 (8)
γ, deg	90	90	99.04 (8)
V, Å^3	1826.3 (8)	2172.7 (9)	639.9 (6)
Z	4	4	1
D(measd), g·cm^{-3}	1.329 (1)	1.487 (1)	1.470 (1)
D(calcd), g·cm^{-3}	1.340	1.499	1.535
abs coeff, cm^{-1}	7.39	9.36	15.19
crystal size, mm	0.2 × 0.6 × 0.2	0.3 × 0.5 × 0.1	0.2 × 0.4 × 0.6
T, °C	18	18	18
data range, deg	$2° \le 2\theta \le 130°$	$2° \le 2\theta \le 130°$	$2° \le 2\theta \le 130°$
scan speed (2θ), deg·min^{-1}	3	3	3
scan range (θ), deg	1.1 + 0.15 tan θ	1.3 ± 0.15 tan θ	1.2 ± 0.15 tan θ
data collected	$h,k,\pm l$	$h,k,\pm l$	$h,\pm k,\pm l$
no. of obsd data	3186	3840	2166
no. of data with $F_o \neq 0.0$	2683	2448	2165
no. of variables	648	490	498
coeff used for refinement			
a	0.3863	0.0	0.7828
b	−0.0297	−0.2358	−0.0261
c	0.0023	0.0459	0.0066
R	0.085	0.166	0.057
R_w	0.070	0.226	0.076
S	1.50	1.31	1.88

We have already reported on the ^1H NMR spectroscopic results of these systems.[8] In this paper we describe X-ray crystallographic studies. The model systems used are as follows: 7-methyl-9-ethylguanine (m^7GuA)–indole-3-acetic acid (IAA) complex, 7-methylguanosine (m^7GuO)–indole-3-acetic acid (IAA) complex, 7-methylguanosine 5′-monophosphate (m^7GMP)–tryptamine (TRP) complex. The chemical formulas are shown in Figure 1, together with the atomic numbering scheme used for X-ray studies. The preliminary X-ray results for m^7GuA–IAA[9] and m^7GMP–TRP[10] complexes have already been reported.

Experimental Section

Syntheses and Crystallization. IAA, TRP, and other tryptophan derivatives were obtained from Sigma Chemical Co. m^7GuA iodide, m^7GuO iodide, and m^7GMP formate were chemically synthesized according to the procedures described previously.[8] These salts, dissolved in water (1% solution), were converted to the OH forms by using a column of Amberlite IRA-401 anion-exchange resin. An equimolar quantity of tryptophan derivatives dissolved in ethanol was then added to the solution. The mixed solution was evaporated to dryness under vacuum. Among many combinations of solvents and of tryptophan derivatives, the complex crystals suitable for X-ray analyses were obtained by the slow evaporation of the following solutions (ca. 2×10^{-4} M) at room temperature (20 °C): 50% aqueous EtOH for the m^7GuA–IAA complex, water–EtOH–hexylene glycol (2:2:1, v/v/v) for the m^7GuO–IAA complex, 70% aqueous MeOH for the m^7GMP–TRP complex.

Crystal Data and Intensity Collection. Details of crystal data for respective complexes and their intensity collection parameters are sum-

(3) (a) Hélène, C.; Maurizot, J. C. *CRC Crit. Rev. Biochem.* **1981**, *10*, 213–258. (b) Hélène, C.; Lancelot, G. *Prog. Biophys. Mol. Biol.* **1982**, *39*, 1–68.
(4) Pullman, B.; Pullman, A. *Proc. Natl. Acad. Sci. U.S.A.* **1958**, *44*, 1197–1202.
(5) Ishida, T.; Shibata, M.; Fujii, K.; Inoue, M. *Biochemistry* **1983**, *22*, 3571–3581.
(6) (a) Wladerkiewicz, R.; Walter, Z.; Reimschussel, W. *Acta Biochim. Pol.* **1986**, *33*, 73–85. (b) Lawley, P. D.; Shah, S. A. *Chem.-Biol. Interact.* **1973**, *7*, 115–120. (c) Lawley, P. D.; Shah, S. A. *Biochem. J.* **1972**, *128*, 117–132. (d) Singer, B.; Fraenkel-Conrat, H. *Biochemistry* **1969**, *8*, 3260–3266.
(7) Furuichi, Y.; Miura, K. *Nature (London)* **1975**, *253*, 374–375.
(8) Kamiichi, K.; Doi, M.; Nabae, M.; Ishida, T.; Inoue, M. *J. Chem. Soc., Perkin Trans. 2* **1987**, 1739–1745.
(9) Ishida, T.; Katsuta, M.; Inoue, M.; Yamagata, Y.; Tomita, K. *Biochem. Biophys. Res. Commun.* **1983**, *115*, 849–854.
(10) Kamiichi, K.; Danshita, M.; Minamino, N.; Doi, M.; Ishida, T.; Inoue, M. *FEBS Lett.* **1986**, *195*, 57–60.

Table II. Selected Torsion Angles of m^{7}GuA–IAA, m^{7}GuO–IAA, and m^{7}GMP–TRP Complexes

	m^{7}GuA–IAA		m^{7}GuO–IAA		m^{7}GMP–TRP
torsion angle	IAA(I)	IAA(II)	IAA(I)	IAA(II)	TRP
C2–C3–C10–C11: χ	111.3 (7)	87.0 (8)	10 (4)	2 (4)	−5.0 (5)
C9–C3–C10–C11	−68.3 (8)	−91.1 (7)	−177 (2)	174 (3)	174.9 (3)
C3–C10C11–O12: ϕ	−13.1 (8)	0.9 (8)	−95 (3)	−111 (3)	
C3–C10–C11–O13	169.8 (5)	−179.0 (5)	86 (3)	73 (3)	
C3–C10–C11–N12: ϕ					−170.0 (3)
	m^{7}GuA–IAA		m^{7}GuO–IAA		m^{7}GMP–TRP
torsion angle	m^{7}GuA(I)	m^{7}GuO(II)	m^{7}GuO(I)	m^{7}GuO(II)	m^{7}GMP
C8–N9–C1′–C2′[a]	2.5 (9)	−14 (1)	5 (3)	3 (3)	−50.5 (4)
C4–N9–C1′–C2′[a]	−179.8 (5)	170.3 (6)	177 (2)	174 (2)	138.4 (3)
C8–N9–C1′–O4′			117 (2)	117 (2)	66.8 (4)
C4–N9–C1′–O4′: χ_{CN}			−71 (2)	−71 (3)	−104.2 (3)
C4′–O4′–C1′–C2′: ν_0			−33 (2)	−38 (2)	−25.2 (3)
O4′–C1′–C2′–C3′: ν_1			45 (2)	44 (2)	39.8 (3)
C1′–C2′–C3′–C4′: ν_2			−39 (2)	−33 (2)	−38.6 (3)
C2′–C3′–C4′–O4′: ν_3			19 (2)	13 (2)	25.2 (3)
C3′–C4′–O4′–C1′: ν_4			9 (2)	16 (2)	−0.1 (3)
P			151	140	161.5
ν_{max}			45	43	40.7
O3′–C3′–C4′–C5′: δ			140 (2)	134 (2)	152.0 (3)
C3′–C4′–C5′–O5′: γ			44 (3)	51 (2)	45.6 (4)
O4′–C4′–C5′–O5′: γ'			−72 (2)	−68 (2)	−72.8 (3)
C4′–C5′–O5′–P: β					−179.8 (2)
C5′–O5′–P–O3P: α					166.1 (2)

[a] The torsion angles for m^{7}GuA are C8–C9–C10–C11 and C4–C9–C10–C11, respectively.

marized in Table I. The unit cell dimensions were determined by a least-squares fit of 2θ angles for 25 reflections ($30° < 2\theta < 60°$) measured with a graphite-monochromated Cu Kα radiation (λ = 1.5418 Å) on an automated Rigaku AFC-5 diffractometer. Intensities for each crystal were collected in a similar manner: a single crystal, sealed in a glass capillary tube under the presence of some mother liquids, was mounted on a goniometer, and the intensity data were collected with the same diffractometer at 40 kV and 180 mA. The ω–2θ scan technique was employed for the intensity recording, where the background was counted for 5 s at both extremes of the peak. Four standard reflections were monitored every 100-reflection interval throughout the data collection and, except for the m^{7}GuO–IAA complex, showed a random variation of ±4% with no significant trends; as those of the m^{7}GuO–IAA complex decreased proportionally to the radiation time, the intensities were corrected on the basis of the decreasing curve. Lorentz and polarization corrections were applied for the intensity data, but no corrections for the absorption and extinction effects were made for either complex.

Structure Solution. m^{7}GuA–IAA Complex. Taking advantage of the ring orientation from a Patterson map, the structure was finally obtained by a direct method (program MULTAN 78[11]).

m^{7}GuO–IAA Complex. By reference to the molecular arrangement observed in guanosine dihydrate,[12] the chemically reasonable structures were finally obtained from an E map generated by a new multiple random start single-solution program (SHELX-86).[13]

m^{7}GMP–TRP Complex. The structure was solved by the combination of heavy atom and direct methods (program MULTAN 78).

Structure Refinement. Refinements for m^{7}GuA–IAA and m^{7}GMP–TRP complexes were performed in a similar manner: positional parameters of non-hydrogen atoms were first refined by a full-matrix least-squares method with isotropic thermal parameters and then by a block-diagonal least-squares method with anisotropic ones. Geometrically reasonable hydrogen atom positions were determined on a difference Fourier map and were included in subsequent refinements with isotropic thermal factors. On the other hand, the structure of the m^{7}GuO–IAA crystal was refined by a full-matrix least-squares method with isotropic thermal factors because of the relatively poor quality of X-ray data due to the fragile and thin-layered crystal. The hydrogen atoms were fixed at the idealized, calculated positions with a common isotropic thermal parameter (B = 3.59 Å^2) and included in the calculations of structure factors, but not in the refinement. The function minimized was $\sum w(|F_o| - |F_c|)^2$, where $|F_o|$ and $|F_c|$ are the observed and calculated structure amplitudes. The weighting scheme used was as follows: $w = a$ for $F_o = 0.0$, and $w = 1.0/[\sigma(F_o)^2 + b|F_o| + c|F_c|^2]$ for $F_o > 0.0$, where $\sigma(F_o)^2$ is the standard deviation of the intensity based on counting statistics. The coefficients a–c are given in Table I. Final R ($=\sum||F_o| - |F_c||/\sum|F_o|$), R^w ($=[\sum w(|F_o| - |F_c|)^2/\sum w|F_o|^2]^{1/2}$), and S ($=[\sum w(|F_o| - |F_c|)^2/(M - N)]^{1/2}$, where M and N are the numbers of reflections and variables, respectively) are also tabulated. Final atomic parameters have been deposited as supplementary material. For all crystallographic computations, the UNICS programs[14] were used, and the atomic scattering factors and the terms of anomalous dispersion corrections were taken from ref 15.

Molecular Orbital Calculations. The atomic charges, the dipole moments, and the HOMO and LUMO energies and their atomic coefficients of 7,9-dimethylguanine and 3-methylindole were calculated by the CNDO/2 method.[16] Their atomic coordinates were derived from the present crystal structures. The stabilities of the respective electronic energies were used to check for convergence in the iteration calculations.

The numerical calculations were performed on an ACOS computer at the Computation Center or at the Crystallographic Research Center, Institute for Protein Research, Osaka University.

Results and Discussion

Molecular Structures. Molecular Dimensions and Planarities. The summation of bond lengths and angles has been deposited as supplementary material, where two crystallographically independent molecules are labeled I and II. The average standard deviations for bond lengths and angles are 0.007 Å and 0.5° for the m^{7}GuA–IAA, 0.03 Å and 2° for the m^{7}GuO–IAA, and 0.004 Å and 0.3° for the m^{7}GMP–TRP complexes, respectively; owing to the high R value, these values for the m^{7}GuO–IAA complex are relatively large, and therefore their bonding parameters are somewhat imprecise. Although some values for the same chemical groups in these complexes are a little different from one another, the quoted values within their estimated standard deviations all seem to be in the usual region, as compared with the related data.[17]

(11) Main, P.; Hull, S. E.; Lessinger, L.; Germain, G.; Declercq, J. P.; Woolfson, M. M. *MULTAN 78, a System of Computer Programs for the Automatic Solution of Crystal Structure from X-ray Diffraction Data*; University of York: York, England, 1978.

(12) Thewalt, U.; Bugg, C. E.; Marsh, R. E. *Acta Crystallogr., Sect. B: Struct. Crystallogr. Cryst. Chem.* **1970**, *B26*, 1089–1101.

(13) Sheldrick, G. M. In *Crystallographic Computing 3*; Sheldrick, G. M., Kruger, C., Goddard, R., Eds.; Oxford University: Oxford, England, 1985; pp 175–189.

(14) *The Universal Crystallographic Computing System-Osaka*; The Computation Center, Osaka University: Osaka, Japan, 1979.

(15) *International Tables for X-ray Crystallography*; Kynoch: Birmingham, England, 1974; Vol. IV.

(16) Pople, J. A.; Segal, G. A. *J. Chem. Phys.* **1966**, *44*, 3289–3296.

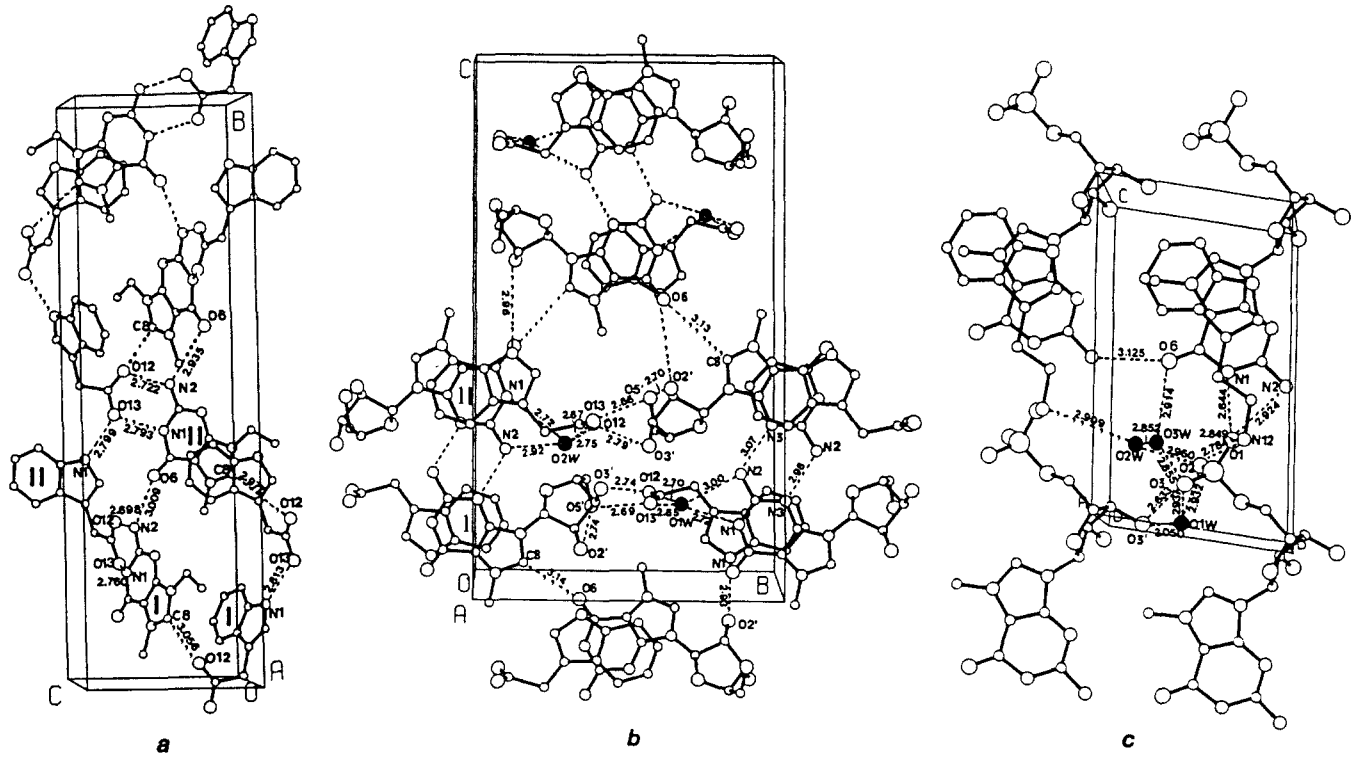

Figure 2. Crystal-packing and hydrogen-bonding modes in the crystal structures of m^{7}GuA–IAA (a), m^{7}GuO–IAA (b), and m^{7}GMP–TRP (c) complexes. The hydrogen bond distances are also shown. Filled circles represent waters of crystallization.

The carboxyl groups of IAA complexed with m^{7}GuA and m^{7}GuO molecules all have demensions corresponding to[18]

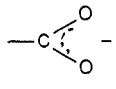

The geometrical data for the phosphate group of m^{7}GMP show the dianion form (OPO_3^{2-}).[17a,b] This dianion is neutralized by the quaternization of a guanine N7 atom and by the NH_3^+ formation of a TRP side chain.[19]

The atomic deviations (in angstroms) from respective best planes for guanine bases, indole rings, and carboxyl groups, together with the dihedral angles between the planes, have also been deposited as supplementary material. These planes are essentially planar with slight deviations (<0.08 Å).

Molecular Conformations. The conformational torsion angles are given in Table II.[20]

(1) IAA and TRP. The χ, ϕ torsion angles of two IAA molecules complexed with m^{7}GuA are both near to the anti-clinal, syn-periplanar region. This conformation has most frequently been found in the crystal structures of IAA alone (χ = 113.4°, ϕ = −11.7°)[21] and complexed with biogenic amines.[17c] On the other hand, two IAA molecules complexed with m^{7}GuO both showed an unusual syn-periplanar, anti-periplanar conformation for their χ, ϕ torsion angles. Although this conformation is energetically more unstable by 7–8 kcal/mol[22] than the usual conformation, it has often been observed in crystals such as the IAA–1-methylnicotinamide complex,[23] where the IAA molecule significantly interacts with the acceptor molecule.

The χ, ϕ torsion angles of TRP complexed with m^{7}GMP took a syn-periplanar, anti-periplanar conformation, consequently forming an extended trans zig-zag chain making a C9–C3–C10–C11–N12 bond sequence. Similar conformation has also been found in the serotonin–creatinine complex crystal,[24] where both molecules strongly interact with each other.

(2) m^{7}GuA, m^{7}GuO, and m^{7}GMP. Generally, the alkyl side chain attached to a bulky hydrophobic aromatic ring shows a tendency to take a torsion angle near to ±90° at the covalent bond. The C8–N9–C10–C11 and C4–N9–C10–C11 torsion angles of m^{7}GuA in its iodide crystal were −93 and 95°, respectively.[25] Despite this conformational preference, both m^{7}GuA molecules adopt an unfavorable syn-periplanar conformation, almost lying on the guanine base. This would be a consequence of the stacking interaction with the IAA molecule (discussed later).

Two crystallographically independent m^{7}GuO molecules show almost similar conformations; the relative orientation of the base with respect to the ribose ring are in a high-anti region (χ_{CN} = −71°) with C2′-endo [m^{7}GuO(I)] or C1′-exo-C2′-endo [m^{7}GuO(II)] envelope sugar puckering. Judging from a χ, P conformational energy map,[26] the m^{7}GuO conformations observed are energetically stable. The orientations about the exocyclic C4′-C5′ bond with respect to the sugar ring take both the same gauche–gauche (gg) conformations. Since the energy gap between the C2′-endo and C1′-exo-C2′-endo ribose puckerings is negligible,[27] the fundamental conformation for the observed m^{7}GuO molecules can be described as the high-anti–C2′-endo–gg form.

(17) (a) Saenger, W. *Principles of Nucleic Acid Structure*; Springer-Verlag: New York, 1984. (b) Taylor, R.; Kennard, O. *J. Mol. Struct.* **1982**, *78*, 1–28. (c) Ishida, T. Dissertation, Faculty of Pharmaceutical Sciences, Osaka University, 1979. (d) Emerson, J.; Sundaralingam, M. *Acta Crystallogr., Sect. B: Structure. Crystallogr. Cryst. Chem.* **1980**, *B36*, 1510–1513.

(18) Weast, R. C., Ed. *Handbook of Chemistry and Physics*; CRC: Cleveland: OH, 1976.

(19) In a preliminary paper[10] the structure of the phosphate group was illustrated as a monoanion form. But, careful consideration of the bonding parameters of this group, after the further structural refinements, led us to the conclusion stated in text.

(20) The conformational torsion angles are defined according to: IUPAC–IUB Commission on Biochemical Nomenclature *Eur. J. Biochem.* **1983**, *131*, 9–15.

(21) Karle, I. L.; Britts, K.; Gum, P. *Acta Crystallogr.* **1964**, *17*, 496–499.

(22) This value was estimated by the CNDO/2 calculations of IAA molecules complexed with m^{7}GuA and m^{7}GuO molecules.

(23) Ishida, T.; Tomita, K.; Inoue, M. *Arch. Biochem. Biophys.* **1980**, *200*, 492–502.

(24) Karle, I. L.; Dragonette, K. S.; Brenner, S. A. *Acta Crystallogr.* **1965**, *19*, 713–716.

(25) Ishida, T.; Katsuta, M.; Inoue, M. *Acta Crystallogr., Sect. C: Cryst. Struct. Commun.* **1984**, *C40*, 439–441.

(26) Saran, A.; Perahia, D.; Pullman, B. *Theor. Chim. Acta* **1973**, *30*, 31–44.

(27) Levitt, M.; Warshel, A. *J. Am. Chem. Soc.* **1978**, *100*, 2607–2613.

Table III

Stacking Parameters for Indole–Guanine Interactions

compd notatn		Figure 3 interactn mode	symmetry operation (indole to guanine at x, y, z)	interplanar spacing, Å	dihedral angle, deg	angle between dipole moments, deg	electrostatic interactn,[a] kcal/mol	stabilizn energy,[b] kcal/mol
m^7GuA–IAA(I)	IA	a, upper	x, y, z	3.435	13.0 (2)	114.5	13.55	−47.63
	IB	a, lower	$x, y, z + 1$	3.554	13.0 (2)	114.5	9.22	−44.74
m^7GuA–IAA(II)	IIA	b, upper	$x - 1, y, z - 1$	3.475	10.4 (2)	113.3	14.96	−43.80
	IIB	b, lower	$x, y, z - 1$	3.568	10.4 (2)	113.3	13.25	−41.73
m^7GuO–IAA(I)	IA	c, upper	x, y, z	3.32	4.2 (7)	39.2	7.92	−43.23
	IB	c, lower	$x + 1, y, z$	3.41	4.2 (7)	39.2	7.08	−42.98
m^7GuO–IAA(II)	IIA	d, upper	x, y, z	3.33	2.7 (7)	45.4	6.64	−43.42
	IIB	d, lower	$x - 1, y, z$	3.46	2.7 (7)	45.4	7.77	−44.30
m^7GMP–TRP	A	e, upper	$x, y, z - 1$	3.380	3.8 (1)	110.9	10.99	−39.91
	B	e, lower	$x - 1, y, z - 1$	3.356	3.8 (1)	110.9	12.00	−41.10

Electrostatic and Orbital Interactions for Short-Contact Atomic Pairs

stacking notatn	atomic name		dist, Å	atomic charge		electronic coupling[c]	atomic coeff		orbital coupling[d]	coupling ratio <3.7 Å[e]
	guanine	indole		guanine	indole		LUMO, guanine	HOMO, indole		
					m^7GuA–IAA					
IA (<3.7 Å)	N7	C4	3.606 (8)	0.058	−0.008	+	−0.4967	−0.3307	+	5/5
	N7	C5	3.656 (8)	0.058	−0.027	+	−0.4967	−0.1436	+	
	C8	C4	3.352 (9)	0.189	−0.008	+	0.6919	−0.3307	−	(2/5)
	C8	C5	3.646 (9)	0.189	−0.027	+	0.6919	−0.1436	−	
	C8	C9	3.623 (8)	0.189	−0.019	+	0.6919	−0.4040	−	
IB (<3.6 Å)	N1	C7	3.477 (7)	−0.222	−0.051	−	0.0719	0.3128	+	4/8
	C5	N1	3.526 (7)	−0.114	−0.139	−	−0.1978	−0.4385	+	
	C6	C7	3.316 (8)	0.377	−0.051	+	−0.1925	0.3128	−	(6/8)
	O6	C6	3.543 (8)	−0.326	0.029	+	0.1985	0.2504	+	
	O6	C7	3.479 (7)	−0.326	−0.051	−	0.1985	0.3128	+	
	N7	N1	3.504 (6)	0.056	−0.139	+	0.4980	−0.4385	−	
IIA (<3.6 Å)	N7	C4	3.415 (8)	0.047	−0.012	+	−0.4922	−0.3451	+	6/7
	C7	C4	3.595 (10)	0.056	−0.012	+	−0.0421	−0.3451	+	
	C8	C4	3.582 (9)	0.202	−0.012	+	0.6976	−0.3451	−	(4/7)
	C8	C9	3.424 (8)	0.202	−0.022	+	0.6976	−0.3939	−	
IIB (<3.6 Å)	N1	C7	3.577 (8)	−0.214	−0.048	−	0.2869	0.2947	+	6/11
	C5	C7	3.433 (8)	−0.108	−0.048	−	0.1967	0.2947	+	
	C5	C8	3.508 (8)	−0.108	0.088	+	0.1967	−0.1458	−	(8/11)
	C6	C6	3.448 (9)	0.373	0.012	−	0.1964	0.2767	+	
	C6	C7	3.467 (8)	0.373	−0.048	+	0.1964	0.2947	+	
	C8	N1	3.563 (8)	0.199	−0.136	+	0.6935	−0.4282	−	
	N9	N1	3.555 (7)	−0.045	−0.136	−	−0.3195	−0.4282	+	
					m^7GuO–IAA					
IA (<3.5 Å)	N1	C9	3.33 (3)	−0.202	−0.039	−	−0.0525	−0.4220	+	12/23
	C2	C4	3.49 (4)	0.406	0.004	−	−0.4894	0.3541	−	
	C4	C5	3.43 (4)	0.208	−0.025	+	0.5540	0.2759	+	(17/23)
	C5	C7	3.48 (4)	−0.098	−0.085	−	−0.3783	−0.4117	+	
	C6	C8	3.28 (3)	0.389	0.111	−	−0.1825	−0.4443	+	
	C6	C9	3.32 (3)	0.389	−0.039	+	−0.1825	−0.4220	+	
	O6	N1	3.28 (3)	−0.305	−0.122	−	−0.1860	0.4987	−	
	O6	C8	3.44 (3)	−0.305	0.111	+	−0.1860	−0.4443	+	
	N7	C7	3.34 (4)	0.033	−0.085	+	−0.4429	−0.4117	+	
IB (<3.5 Å)	C2	C4	3.48 (4)	0.409	0.010	−	0.4770	−0.3530	−	8/20
	N3	C4	3.27 (3)	−0.315	0.010	+	−0.0516	−0.3530	+	
	N3	C5	3.45 (4)	−0.315	−0.020	−	−0.0516	−0.2899	+	(15/20)
	C4	C6	3.43 (4)	0.204	0.025	−	−0.5600	0.1701	−	
	C5	C7	3.45 (4)	−0.094	−0.087	−	0.3825	0.4227	+	
	C5	C8	3.45 (3)	−0.094	0.109	+	0.3825	0.4380	+	
	N9	C6	3.37 (4)	0.003	0.025	−	0.4031	0.1701	+	
IIA (<3.5 Å)	N1	C3	3.44 (3)	−0.228	−0.055	−	−0.2713	−0.4655	+	12/22
	N1	C9	3.42 (3)	−0.228	0.022	+	−0.2713	−0.3163	+	
	N3	C4	3.49 (3)	−0.328	−0.040	−	0.0551	0.3876	+	(16/22)
	C4	C5	3.45 (4)	0.236	0.015	−	−0.5704	0.4064	−	
	C5	C7	3.45 (3)	−0.086	−0.030	−	0.1860	−0.2284	−	
	C6	C8	3.39 (3)	0.371	0.052	−	0.1890	0.2782	+	
	O6	N1	3.34 (3)	−0.322	−0.086	−	−0.1812	0.3116	−	
	N7	C7	3.46 (3)	0.046	−0.030	+	−0.4881	−0.2284	+	
IIB (<3.5 Å)	N3	C4	3.45 (3)	−0.322	−0.041	−	−0.0554	−0.3900	+	11/19
	C4	C4	3.49 (3)	0.240	−0.041	+	−0.5682	−0.3900	+	(15/19)
	C4	C5	3.41 (4)	0.240	0.012	−	−0.5682	−0.4230	+	
	O6	N1	3.47 (3)	−0.312	−0.082	−	0.1951	−0.3100	−	
	N7	C7	3.46 (3)	0.034	−0.030	+	0.4857	0.2247	+	
	N9	C6	3.49 (3)	−0.031	−0.020	−	0.3292	0.3683	+	

Table III (Continued)

Electrostatic and Orbital Interactions for Short-Contact Atomic Pairs

stacking notatn	atomic name guanine	atomic name indole	dist, Å	atomic charge guanine	atomic charge indole	electronic coupling[c]	atomic coeff LUMO, guanine	atomic coeff HOMO, indole	orbital coupling[d]	coupling ratio <3.7 Å[e]
					m^{7}GMP–TRP					
A (<3.5 Å)	N1	C3	3.500 (5)	−0.205	−0.038	−	−0.2920	−0.4849	+	13/25
	N1	C10	3.407 (4)	−0.205	−0.010	−	−0.2920	0.1207	−	
	C5	C9	3.426 (5)	−0.110	−0.017	−	−0.1981	−0.3753	+	(17/25)
	O6	C4	3.472 (5)	−0.335	0.002	+	0.2048	0.3514	+	
	C7	C5	3.376 (6)	0.053	−0.031	+	0.0426	0.1788	+	
	C8	C7	3.390 (5)	0.191	−0.053	+	−0.6897	−0.3170	+	
B (<3.5 Å)	N1	C3	3.446 (5)	−0.205	−0.035	−	0.2917	−0.4811	−	11/24
	N1	C10	3.464 (4)	−0.205	−0.011	−	0.2917	0.1205	+	
	C2	C2	3.381 (5)	0.420	0.050	−	−0.4964	−0.3757	+	(18/24)
	N3	N1	3.482 (4)	−0.306	−0.138	−	−0.0684	0.4528	−	
	N3	C2	3.269 (4)	−0.306	0.050	+	−0.0684	−0.3757	+	
	C4	N1	3.276 (4)	0.249	−0.138	+	0.5692	0.4528	+	
	C4	C2	3.459 (5)	0.249	0.050	−	0.5692	−0.3757	−	
	C4	C8	3.496 (5)	0.249	0.094	−	0.5692	0.1154	+	
	C5	C8	3.441 (5)	−0.109	0.094	+	−0.1977	0.1154	−	
	C5	C9	3.359 (5)	−0.109	−0.018	−	−0.1977	−0.3651	+	
	N7	C8	3.489 (5)	0.045	0.094	−	0.4845	0.1154	+	
	C7	C5	3.435 (6)	0.053	−0.028	+	0.0420	0.1637	+	
	C7	C6	3.476 (6)	0.053	0.014	−	0.0420	−0.2564	−	
	C8	C7	3.384 (5)	0.197	−0.054	+	−0.6903	−0.3139	+	
	N9	N1	3.432 (4)	−0.039	−0.138	−	0.3243	0.4528	+	

[a] Electronic energy (kcal/mol) was computed by $332.0\sum_i\sum_j q_i q_j / r_{ij}$ $(i > j)$, where r_{ij} is the distance (Å) between atom i of the guanine ring and j of the indole ring, and q_i or q_j is the Coulombic charge on atom i or j. [b] Stabilization energy (kcal/mol) was calculated by using the following equation and the total energy (E) of the respective molecules: Stabilization energy = E(stacked pair) − $\sum E$(individual). The E values for the guanine and indole rings were calculated by the CNDO/2 method using 7,9-dimethylguanine and 3-methylindole, respectively. [c] Electronic attraction or repulsion is designed by + or −, respectively. [d] The coupling or splitting interaction between the HOMO and LUMO orbitals is designed by + or −, respectively. [e] The number of electrostatic attractions or orbital coupling (in parentheses) pairs per total number of atomic pairs less than 3.7 Å is shown.

This combination of χ, P, γ torsion angles has frequently been observed in other ribonucleosides.[28]

From the χ_{CN}, P, and γ values listed in Table III, the conformation of m^{7}GMP is best described as the anti–C2′-endo–gg form,[29] and the orientation of the phosphate group to the ribose ring, defined by torsion angle β, is in the most energetically stable anti-periplanar region.[30]

Two m^{7}GuO and m^{7}GMP molecules showed a common feature concerning the nucleoside moiety: (high-)anti–C2′-endo–gg conformation. Therefore, it is of interest to consider to what extent the N7-methylation exerts its effect upon the conformations of guanine nucleoside and nucleotide. A survey of m^{7}GuO-related compounds showed that this conformational characteristics has also been found in guanosine[12] and other related crystals. On the other hand, the two crystallographically independent m^{7}GuO molecules in the iodide crystal[31] showed the coexistence of (anti–C3′-endo–gg) and (syn–C2′-endo–gg) conformers. These facts imply that the χ_{CN} and ribose conformations of guanosine are not significantly effected by the N7-methylation and depend largely on the environment of crystal packing. The gauche–gauche orientation about the C4′–C5′ bond may be a stable conformation for the m^{7}GuO molecule. On the other hand, the anti–C2′-endo–gg conformation observed for m^{7}GMP is conceivable as a favored form, because m^{7}GMP complexed with L-phenylalanine[32] has shown the same conformation. But this conformation has also been found in GMP crystal structures such as Cu^{II}GMP[33] and Na_2GMP.[34] Therefore, it could not be concluded that the "rigid" conformation observed in m^{7}GMP results from N7-methylation, although the possibility of N7-methylation shifting the equilibrium among various GMP conformers toward the anti–C2′-endo–gg form cannot be disregarded. This conflicts with the solution study,[35] in which it has been concluded that N7-methylation of GMP causes a rigid anti–C3′-endo–gg conformation. It is of interest to note that, in contrast to m^{7}GMP, GMP protonated at N7 shows this conformation.[17d]

Crystal Packings and Hydrogen Bonds. The schematic drawings of the crystal packings are shown in Figure 2, where the dotted lines represent hydrogen bonds. The details of hydrogen bonding parameters are available as supplementary material.

m^{7}GuA–IAA Complex. A characteristic observed in this crystal structure is the formation of two kinds of stacking layers consisting of alternate guanine and indole rings. These layers are piling up along the a and c directions and therefore fall almost at right angles to each other (95.9°). The hydrogen bonding modes of m^{7}GuA–IAA(I) are completely the same as those of -(II). The participation of a guanine C8 atom in the hydrogen bond formation is a consequence of the base methylation: the CNDO/2 calculations showed the increased bonding ability of C8–H hydrogen (−0.011 eu at the GuA H8 atom and 0.075 eu at m^{7}GuA). Indeed, this type of hydrogen bond has been found in m^{7}GuA iodide,[25] m^{7}GuO–IAA, and m^{7}GuO iodide[31] crystals, and the lability of the H8 proton has also been observed in the solution state.[8]

Another characteristic observed in this crystal is the hydrogen bonds between the carboxyl group and the guanine base, and this provides a good model for the specific recognition of the guanine base in the single-stranded nucleic acid by an acidic amino acid such as Asp or Glu. These paired planes are approximately coplanar with the dihedral angle of 8.3 (3)° for the guanine-

(28) de Leeuw, H. P. M.; Haasnoot, C. A. G.; Altona, C. *Isr. J. Chem.* **1980**, *20*, 108–126.

(29) In an preliminary paper[10] we reported that the conformation of m^{7}GMP is the anti–C2′-exo–gg form. But, this was a mistake.

(30) Saran, A.; Pullman, B.; Perahia, D. *Biochim. Biophys. Acta* **1973**, *299*, 497–499.

(31) Yamagata, Y.; Fukumoto, S.; Hamada, K.; Fujiwara, T.; Tomita, K. *Nucleic Acid Res.* **1983**, *11*, 6475–6486.

(32) Ishida, T.; Kamiichi, K.; Kuwahara, A.; Doi, M.; Inoue, M. *Biochem. Biophys. Res. Commun.* **1986**, *136*, 294–299. To our knowledge, this complex is the only X-ray example for m^{7}GMP molecule.

(33) Clark, G. R.; Orbell, J. D.; Aoki, K. *Acta Crystallogr., Sect. B*: **1978**, *B34*, 2119–2128.

(34) (a) Katti, S. K.; Seshdri, T. P.; Viswamitra, M. A. *Acta Crystallogr., Sect. B: Struct. Crystallogr. Cryst. Chem.* **1981**, *B37*, 1825–1831. (b) Barnes, C. L.; Hawkinson, S. *Acta Crystallogr., Sect. B: Struct. Crystallogr. Cryst. Chem.* **1982**, *B38*, 812–817.

(35) (a) Hickey, E. D.; Weber, L. A.; Baglioni, C.; Kim, C. H.; Sarma, R. H. *J. Mol. Biol.* **1977**, *109*, 173–183. (b) Kim, C. H.; Sarma, R. H. *J. Am. Chem. Soc.* **1978**, *100*, 1571–1590.

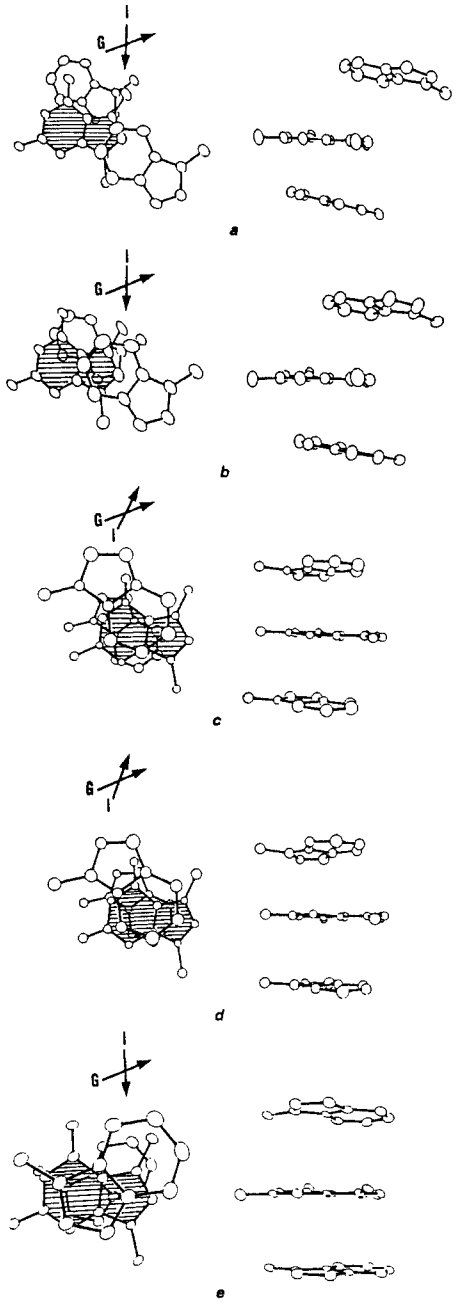

Figure 3. Stacking interaction modes of indole–guanine systems. The central guanine base is shown by oblique lines.

(I)–carboxyl(II) pair and 22.2 (3)° for the guanine(II)–carboxyl(I) pair.

m^{7}GuO–IAA Complex. A remarkable feature in this crystal packing is that two crystallographically independent m^{7}GuO–IAA complex pairs are almost related by diad symmetry. This pseudosymmetry, however, forms an angle of 110.13° with the 0, 1, 1 plane, and this is the reason why this crystal does not take an orthorhombic space group. Because of the pseudodiad symmetry between the two complex pairs, the hydrogen-bonding patterns are completely the same. Both m^{7}GuO(I) and -(II) are base-paired via two N2–H···N3 hydrogen bonds (these paired bases are nearly coplanar with a dihedral angle of 11.3 (6)°), and this pairing is further stabilized by the ionic interactions between N2 and O1′ atoms of m^{7}GuO molecules (N2···O1′ = 3.03 (2) Å).

m^{7}GMP–TRP Complex. The stacking layers consisting of alternate indole and guanine rings run along the *a* axis. The ribose and phosphate groups of m^{7}GMP and the aminoethyl group of TRP jut out from the layers. Each oxygen atom of the anionic phosphate group participates in three hydrogen bonds as an electron acceptor. The TRP molecule is linked with m^{7}GMP by two hydrogen bonds of N12I···O2P and N12I···O3P.[36] The waters of crystallization are located at the cavities formed by the crystal packing of the m^{7}GMP–TRP complex, and each of them stabilizes this complex by three hydrogen bond formations with neighboring donor or acceptor atoms.

Stacking Interaction between the Indole Ring and Guanine Base. As is obvious from Figure 2, the most pronounced structural feature commonly found in these m^{7}G–indole systems is the extensive stacking formation between the indole ring and the guanine base. Parameters for their stacking interactions are summarized in Table III. Figure 3 illustrates the stacking modes between the indole and guanine rings, where the two up-and-down stacked indoles are projected perpendicular or parallel to the central guanine base. This figure also shows the vectors of respective aromatic dipole moments, represented by arrows above the respective figures (I, indole; G, guanine).

m^{7}GuA–IAA Complex. The indole–guanine stacking modes are shown in Figure 3a and b. There are two kinds of stacking modes of indole rings with respect to the central guanine ring for each complex pair. The dihedral angles between the stacked rings are 13.0 (2) and 10.4 (2)° for both pairs of complex pairs (I) and (II), respectively. The averaged interplanar spacings are 3.435 and 3.554 Å for the upper and lower pairs of (I), and 3.475 and 3.568 Å for those of (II), respectively. The slight, but significant deviation from the parallel stacking, the interplanar spacing distance slightly longer than the normal van der Waals separation distance (=3.4 Å), and the relatively small overlapping area indicate that these stacking interactions are stabilized by the van der Waals contacts between the two respective aromatic rings; their stabilization energies caused by the stacking formations are in the range of −42 to −48 kcal/mol.

m^{7}GuO–IAA Complex. By analogy with the m^{7}GuA–IAA complex pairs, four kinds of indole–guanine stacking modes exist, as shown in Figure 3c and d. But the stacking parameters are significantly different from m^{7}GuA–IAA. The indole rings are stacked almost parallel on the guanine base [4.2 and 2.7° for complex pairs (I) and (II)], and two of four averaged interplanar spacings [3.32 and 3.33 Å for the upper pairs of (I) and (II)] are meaningfully shorter than the separation distance 3.4 Å. Such a parallel stacking arrangement with an interplanar spacing of less than 3.4 Å, together with no direct hydrogen bond formation between the aromatic rings, clearly shows that, in addition to normal van der Waals forces, both aromatic rings are stabilized by the forces caused by partial charge transfer from the HOMO of the indole ring to the LUMO of the guanine base, even in their ground states. The extensive stacking of the upper and lower indole rings to the central guanine base is also an indication of the π–π charge-transfer interaction, because the larger the overlapping area between the donor and the acceptor, the stronger the interaction becomes. These stacking parameters have commonly been observed in typical charge-transfer complexes such as indole–nicotinamide[23] and indole–flavin[37] systems.

m^{7}GMP–TRP Complex. The stacking parameters for this complex are nearly the same as those for the m^{7}GuO–IAA ones: both the upper and lower indole rings are stacked on the central guanine base with the almost parallel alignment [dihedral angle, 3.8 (1)°] and with interplanar spacing shorter than 3.4 Å (3.380 and 3.356 Å for upper and lower pairs). Thus, the π–π charge-transfer force could be thought of as being a major factor stabilizing the molecular association of these complex pairs.

Effect of Ribose Ring and Phosphate Group for Indole–Guanine Stacking Interaction. As is obvious from Table III and Figure 3, the ribose ring and phosphate group appear to strengthen the indole–guanine stacking interaction. Comparison of the stacking parameters indicates that the interaction of m^{7}G derivatives to the indole ring increases in the following order: m^{7}GMP ≥ m^{7}GuO

(36) The N1 atom of TRP did not participate in hydrogen bond formation. The nearest neighboring acceptor atom was the O2′ atom of m^{7}GMP, with N1···O2′ (x + 1, y, z + 1) = 3.328 (4) Å, H1···O2′ = 2.55 (6) Å, and N1–H1···O2′ = 144 (5)°.

(37) Inoue, M.; Shibata, M.; Kondo, Y.; Ishida, T. *Biochemistry* **1981**, *20*, 2936–2945.

> m^7GuA. As was already stated in the introduction, the stacking interaction takes place between the HOMO of the indole ring and the LUMO of the guanine base. Therefore, the ribose and phosphate groups appear not to directly affect the interaction but to provide an environment suitable for the stacking formation. The existence of these groups restricts the rotation of the guanine base via the glycosyl bond connection. Consequently, the interaction area of the indole ring allowed to interact with the guanine base will be quite limited, compared with the case of the m^7GuA–IAA complex. The stable stacking mode once formed, which may be further stabilized by the hydrogen bond formations between the base and the ribose or phosphate group, will be held in spite of an environmental change, such as from a solution → solid state. This idea can account for the reason why the stacking modes observed in m^7GuO–IAA and m^7GMP–TRP complexes are more compact and stable than those in m^7GuA–IAA; in other words, the stacking mode of both aromatic rings is severely controlled by the ribose and/or phosphate group, and only the most stable mode is selected from among many other forms.

It is of interest to note that the interaction order in solution, which was shown by NMR analyses,[8] is inconsistent with that in the solid state: $m^7GMP > m^7GuA > m^7GuO$. However, we can account for this conflict as follows: contrary to the solid state, the NMR data in solution are time-averaged data for various stacking interaction modes. Therefore, even though some of the stacking species in the m^7GuO–tryptophan complex are much more stable than those in m^7GuA–tryptophan, the overall interacting species are much more predominant for the latter complex because of the lack of the bulky ribose ring. On the other hand, the preference of m^7GMP in the interaction with tryptophan would be mainly due to the electrostatic interactions between the anionic phosphate and the cationic tryptophan side chain atoms.

Ring Orientation in Indole–Guanine Stacking Interaction. It is well-known that the dipole–(induced) dipole and electrostatic interactions are largely responsible for specifying the mutual orientation of two associated molecules. As is obvious from Figure 3, however, the dipole–dipole interaction is not important for determining the mutual orientation between the indole and guanine rings. The directions of the aromatic dipole moments for m^7GuA–IAA and m^7GMP–TRP complexes are almost at right angles (indicating little of its interaction), and those for m^7GuO–IAA complexes show repulsion. As is shown in Table III, on the other hand, the electrostatic or HOMO (indole)–LUMO (guanine) interaction is likely to be important for controlling the mutual orientation. Although total electrostatic energies for respective stacked pairs all have positive values and are therefore unfavorable as the total stacking force, many of the short-contact atomic pairs in m^7GuA–IAA (IA, IIA) occur between two atoms capable of forming an electron-rich and electron-deficient pair. This means that the ring orientations of IA and IIA complex pairs are determined by the electrostatic interactions. On the other hand, as the overlapping area of both rings becomes extensive, the HOMO–LUMO interactions serve as an important factor for determining the mutual orientation. As can be seen in m^7GuA–IAA (IB, IIB), m^7GuO–IAA, and m^7GMP–TRP stacking pairs of Table III, the atomic coefficients between the HOMO of the indole ring and the LUMO of the guanine ring have mostly the same signs in the short contact atomic pairs, and they are interactive with each other due to the coupling of their orbitals. The importance of HOMO–LUMO interactions for determining the ring orientation has also been noted in indole–adenine,[5] flavin[37], pyridinium,[38] and thiamin.[39]

Biological Significance of Indole–Guanine Stacking Interaction. An important biological insight gained by the present X-ray studies is that the strong stacking interaction via partial π–π charge-transfer interaction can be formed between the indole ring of tryptophan and the guanine base of nucleic acid. The importance of the stacking interaction of tryptophan with the nucleic acid base in specific protein–nucleic acid recognition has been suggested for some time; for example, the damage recognition and catalytic activity of DNA endonucleases for apurinic/apyrimidinic sites are monitored via the stacking interaction of model peptide Lys-Trp-Lys and nucleic bases,[40] and the binding of gene 32 protein (from page T4) to single-stranded DNA necessitates the stacking interaction of the tryptophan residue with the nucleic bases.[41] Nevertheless, the stacking structure between the tryptophan and the neutral nucleic base has not yet been observed in the crystalline state, probably due to its weak interaction force. Here we want to emphasize that the stacking interaction is significantly strengthened by the protonation of the nucleic base, and the present stacking examples are a good model for the interaction of tryptophan with the protonated guanine base. Because of the high nucleophilicity of the guanine N7 atom, protonation at this atom is highly likely to take place in an acidic or neutral nucleic acid,[42] and the guanine base may become the most susceptible target for specific recognition by the tryptophan residue. Such a circumstance exists in the living cell.

On the other hand, it is known that the alkylation of DNA by chemical mutagens mainly takes place at the N7 atom of the guanine base, whether DNA takes a single-stranded or double-helical structure.[6] The alkylated (therefore damaged) nucleic acid must be renatured with various repairing enzymes. Although these repair mechanisms are not well analyzed, the present results may shed light on the problem of how the enzymes recognize the alkylated nucleic bases specifically.

Another biologically important insight obtained from this study is the account of the structural role of the mRNA cap structure $m^7G(5')ppp(5')N$. Many biological experiments have demonstrated that the cap structure influences eukaryotic mRNA maturity, stability, and protection from degradation and, more importantly, plays a role in the initiation of protein synthesis, which is mediated by protein factors, including a cap binding protein (CBP).[43] Many studies on the cap structure–function relationship have provided the following insights: (1) the cap structure of mRNA is specifically recognized by CBP,[44] (2) this specific recognition is competitively inhibited by m^7GMP analogues,[45] (3) for this inhibitory activity, the positive charge of the guanine N7 atom is absolutely necessary,[46] (4) the guanine N2 amino group is also important for effective capped mRNA–CBP binding.[46] These insights clearly show that the amino acid(s) in CBP participate in the specific binding with the m^7G base of the cap structure. Provided that the tryptophan residues are responsible for this role, the strong stacking interactions between the indole and guanine rings observed in the present studies can well account for the experimental facts of (1)–(3). Furthermore, the specific hydrogen bonds between the carboxyl group and the N1 and N2 atoms of the guanine base found in m^7GuA–IAA complexes, as a model for the binding mode between the capped m^7G base and

(38) Ishida, T.; Ibe, S.; Inoue, M. *J. Chem. Soc., Perkin Trans. 2* **1984**, 297–304.

(39) Ishida, T.; Matsui, M.; Inoue, M.; Hirano, H.; Yamashita, M.; Sugiyama, K.; Sugiura, M.; Tomita, K. *J. Am. Chem. Soc.* **1985**, *107*, 3305–3314.

(40) (a) Duker, N. J.; Hart, D. M. *Biochem. Biophys. Res. Commun.* **1982**, *105*, 1433–1439. (b) Behmoaras, T.; Toulme, J.-J.; Hélène, C. *Nature (London)* **1981**, *292*, 858–859. (c) Shine, N. R.; James, T. L. *Biochemistry* **1985**, *24*, 4333–4341. (d) Shine, N.; Bubienko, E.; James, T. L. *Biochemistry* **1985**, *24*, 4341–4345.

(41) (a) Toulme, J.-J.; Doan, T. L.; Hélène, C. *Biochemistry* **1984**, *23*, 1195–1201. (b) Prigodich, R. V.; Casas-Finet, J.; Williams, K. R.; Konigsberg, W.; Coleman, J. E. *Biochemistry* **1984**, *23*, 522–529.

(42) Yamauchi, K. *Kagaku no Ryoiki* **1979**, *33*, 523–529.

(43) For reviews, see: (a) Miura, K. *Adv. Biophys.* **1981**, *14*, 205–238. (b) Mizumoto, K.; Kaziro, Y. *Protein, Nucleic Acid Enzyme* **1982**, *27*, 773–793. (c) Miura, K.; Shinozaki, K. *Protein, Nucleic Acid Enzyme* **1985**, *30*, 711–721.

(44) (a) Shatkin, A. J. *Cell* **1985**, *40*, 223–224. (b) Rhoads, R. E. In *Progress in Molecular and Subcellular Biology*; Hahn, F. E., Kopecko, D. J., Muller, W. E. G., Eds.; Springer-Verlag: Berlin, 1985; Vol. 9, pp 104–155.

(45) (a) Shafritz, D. A.; Weinstein, J. A.; Safer, B.; Merrick, W. C.; Weber, L. A.; Hickey, E. D.; Baglioni, C. *Nature (London)* **1976**, *261*, 291–294. (b) Roman, R.; Brooker, J. D.; Seal, S. N.; Marcus, A. *Nature (London)* **1976**, *260*, 359–363. (c) Canaani, D.; Revel, M.; Groner, Y. *FEBS Lett.* **1976**, *64*, 326–331.

(46) (a) Adams, B. L.; Morgan, M.; Muthukrishnan, S.; Hecht, S. M.; Shatkin, A. J. *J. Biol. Chem.* **1978**, *253*, 2589–2595. (b) Darzynkiewicz, E.; Ekiel, I.; Tahara, S. M.; Seliger, L. S.; Shatkin, A. J. *Biochemistry* **1985**, *24*, 1701–1707.

the acidic amino acid(s) in CBP, can also explain the result of (4).[47] Recently, the amino acid sequence of CBP was determined by Rychlik et al.[48] The most unusual feature of the CBP is the high tryptophan content [4.7 mol % (seven residue)], while other initiation factors (eIF-2, -4A, -4B, -4C, 5) vary from 0 to 1 mol % tryptophan.[49] Furthermore, this CBP shows a high content of acidic amino acids (25 and 28 residues for Glu and Asp, respectively). This result adds further weight to the above-mentioned discussions.

Finally, we want to introduce a report[50] that demonstrates the importance of the present results: antibodies specific for methylated DNA elicited in rabbits recognize only a single-strand region of DNA containing m^7G base, and its antigenicity is decreased or lost in parallel with the extent of the release of m^7G residues. This means that m^7G residues of methylated DNA play an important role in forming a characteristic complex with the amino acids of antibody.

The present study clearly shows the importance of the tryptophan residue for selective recognition with the guanine base of nucleic acid. The stacking interactions involving the charge-transfer interactions occur in many biological systems and play a key role in their effective actions.

Acknowledgment. This work was supported by a Grant-in-Aid for Scientific Research from the Ministry of Education, Science, and Culture, Japan (No. 61571037).

Registry No. m^7GuA-IAA, 113111-13-0; m^7GuO-IAA, 113111-14-1; m^7GMP-TRP, 113111-15-2; m^7G, 578-76-7; Trp, 73-22-3.

Supplementary Material Available: Tables of final atomic coordinates with isotropic thermal parameters of non-hydrogen atoms, anisotropic thermal parameters of non-hydrogen atoms (m^7GuA–IAA and m^7GMP–TRP complexes), atomic coordinates and isotropic thermal parameters of hydrogen atoms, bond lengths and angles, least-squares best planes (the atomic deviations from them and the dihedral angles between them), hydrogen bond distances and angles, and ORTEP drawings of molecular conformations and crystal packings (17 pages); tables of observed and calculated structure factors (33 pages). Ordering information is given on any current masthead page.

(47) This type of hydrogen bond has been found in the m^7GMP–L-phenylalanine complex crystals[32] and exists as a predominant form in the solution state: Lancelot, G.; Hélène, C. *Proc. Natl. Acad. Sci. U.S.A.* **1977**, *74*, 4872–4875.

(48) (a) Rychlik, W.; Gardner, P. R.; Vanaman, T. C.; Rhoads, R. E. *J. Biol. Chem.* **1986**, *261*, 71–75. (b) Rychlik, W.; Domier, L. L.; Gardner, P. R.; Hellmann, G. M.; Rhoads, R. E. *Proc. Natl. Acad. Sci. U.S.A.* **1987**, *84*, 945–949.

(49) Grifo, J. A.; Tahara, S. M.; Leis, J. P.; Morgan, M. A.; Shatkin, A. J.; Merrick, W. C. *J. Biol. Chem.* **1982**, *257*, 5246–5252.

(50) Kawarada, Y.; Okuhara, E. *Tohoku J. Exp. Med.* **1986**, *149*, 151–161.

Communications to the Editor

Solid–Liquid Intermolecular Transfer of Dynamic Nuclear Polarization. Enhanced Flowing Fluid ^{1}H NMR Signals via Immobilized Spin Labels

R. Gitti, C. Wild, C. Tsiao, K. Zimmer, T. E. Glass, and H. C. Dorn*

Department of Chemistry, Virginia Polytechnic Institute and State University Blacksburg, Virginia 24061

Received November 30, 1987

Although static dynamic nuclear polarization (DNP) experiments for a number of NMR nuclides (e.g., ^{1}H, ^{13}C, ^{31}P, etc.) are well documented for both liquid[1] and solid[2] samples, a number of limitations are inherent in static DNP experiments. This is notwithstanding the potential utility of DNP for providing large Overhauser enhancements (A) which are ultimately proportional to the magnetogyric ratios of the electron and nuclear spins ($A\alpha\gamma_e/\gamma_n$).[1-5]

In most previous DNP studies, inter- and intramolecular effects have been monitored in both static liquid or solid samples in the presence of the free-radical system. However, for many DNP experiments there are undesirable effects caused by the spin label in situ (e.g., line broadening of the NMR signals). In this communication, we demonstrate intermolecular transfer of the polarization from an immobilized spin label to a flowing fluid bolus. *Thus, the flowing liquid bolus (monitored downstream) represents a messenger spatially removed from the immobilized reporter group (i.e., spin label).*

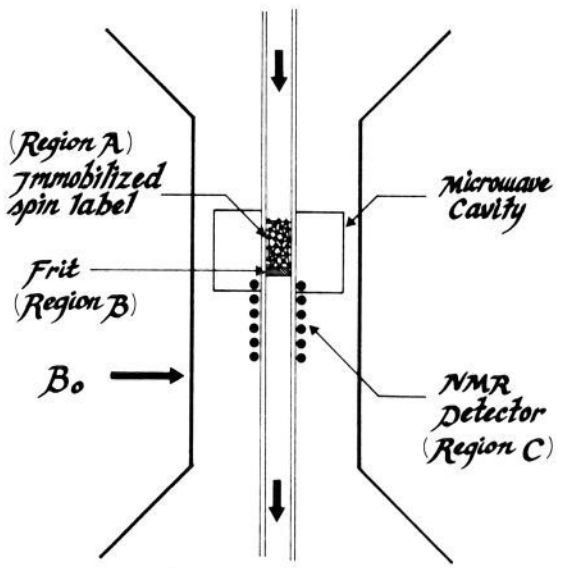

Figure 1. Flow SLIT ^{1}H DNP apparatus. All experiments were performed at $\omega_e/2\pi$ = 9.3 GHz, $\omega_n/2\pi$ = 14.0 MHz, and $B_0 \simeq$ 3.3 kg. A modified Varian E-3 EPR spectrometer with a Hughes TWT amplifier was used to generate ω_e in a standard TE_{102} cavity (region A). A wideband JEOL FX-200 spectrometer console was used to detect the ^{1}H NMR signal induced in region C.

We have recently demonstrated[3] a significant advantage of flow DNP in providing independent optimization of the B_{1s} ESR microwave field and the FT NMR detector. For example, for

(1) For reviews, see: (a) Hausser, K. H.; Stehlik, D. In *Adv. Magn. Reson.* **1968**, *3*, 79. (b) Dwek, R. A.; Richards, R. E.; Taylor, D. *Annu. Rev. NMR Spectrosc.* **1969**, *2*, 293. (c) Müller-Warmuth, W.; Meise-Gresch, K. *Adv. Magn. Reson.* **1983**, *11*, 1.

(2) Wind, R. A.; Duijveshijn, M. J.; Van Der Lugt, C.; Manenshijn, A.; Vriend, J. *Prog. NMR Spectrosc.* **1985**, *17*, 33.

(3) Dorn, H. C.; Wang, J.; Allen, L.; Sweeney, D.; Glass, T. E. *J. Magn. Reson.* **1988**, in press.

(4) Trommel, J. *Ph.*D. Thesis, Delft University of Technology, Delft, Netherlands, 1978.

(5) Natusch, D. F. S.; Richards, R. E.; Taylor, D. *Mol. Phys.* **1966**, *11*, 42.

0002-7863/88/1510-2294$01.50/0